

Finding the remnants of lost jets at RHIC

Subrata Pal¹ and Scott Pratt²

¹*National Superconducting Cyclotron Laboratory and Department of Physics and Astronomy,
Michigan State University, East Lansing, Michigan 48824*

²*Department of Physics and Astronomy, Michigan State University, East Lansing, Michigan 48824*

A fast parton propagating through partonic matter loses energy by medium-induced gluon radiation. We propose a method to detect the energy loss of jets and the final-state interaction of the radiated gluons and the jets with the partonic medium. By embedding jets and radiated energy into a parton cascade, we find that the fate of lost jets can be studied by analyzing the momentum distribution of soft hadrons relative to the jet axis.

PACS numbers: 12.38.Mh, 24.85.+p, 25.75.-q

The attenuation of hard jets produced in pQCD processes provides an excellent opportunity to study the properties of hot and dense partonic matter expected to be formed in ultrarelativistic heavy ion collisions [1, 2, 3, 4]. Due to the energy lost by the jets as a result of multiple elastic and inelastic interactions in the partonic matter, the final hadron p_T distribution from the fragmenting jets will be suppressed compared to that from nucleon-nucleon reference spectra convoluted with the number of binary collisions. Measurement of high p_T hadrons is thus expected to provide a diagnostic tool for the total energy loss ΔE of jets in the dense partonic medium [5, 6]. Relative to the binary collision scaled $p\bar{p}$ reference spectrum, experimental data [7, 8, 9, 10] for central Au+Au collisions at RHIC indeed showed a suppression for π^0 s and h^\pm , where the suppression is smallest at $p_T \approx 2$ GeV/c and increases to an approximately constant value for $p_T = 4 - 10$ GeV/c. Apart from the suppression of high p_T hadrons at RHIC, the suppression of the away-side jets compared to the near-side jets at high p_T [11] is an indication of jet quenching for the away-side jet.

Even the disappearance of away-side jets might be considered as only circumstantial evidence of jet-energy loss. For instance, one could imagine a scenario where monojets are produced due to the $2 \rightarrow 1$ gluon fusion processes, e.g., in the gluon saturation model [12]. If the away-side jet were truly produced then absorbed by the medium, the extra momentum and energy should survive. Our aim is to investigate the degree to which the lost energy and momentum can be extracted from low- p_T observables. We propose a straight-forward strategy of gating on the observation of a high-energy parton, then analyzing the accompanying alteration of the low-energy spectra relative to the azimuthal direction of the jet. The distribution of these extra particles, as a function of p_T and as function of their rapidity and azimuthal angle relative to the triggering jet, might provide critical insight for understanding the mechanism for jet-energy loss.

To investigate these issues, we consider a baseline dynamical model of the collision, onto which hard jets have been embedded. The base distribution consists of the HI-

JING model [13, 14], which is used to generate a set of initial partons, and ZPC, a parton cascade which simulates the subsequent elastic partonic interactions[15]. HIJING provides the initial momentum and space-time coordinates of partons from minijets and strings which originate from soft nucleon-nucleon collisions. The parton-parton elastic scattering in ZPC is determined by the cross section,

$$\frac{d\sigma}{d\hat{t}} = C_a 4\pi\alpha_s^2 \left(1 + \frac{\mu^2}{\hat{s}}\right) \frac{1}{(\hat{t} - \mu^2)^2}, \quad (1)$$

where \hat{t} and \hat{s} are the usual Mandelstam variables, $C_a = 9/8, 1/2, 2/9$ for gg, gq, qq scatterings, and α_s is the strong coupling constant assumed to be 0.30. The effective screening mass μ is assumed to be independent of temperature and density and is used as a parameter to obtain the desired parton-parton elastic cross section $\sigma \approx C_a 4\pi\alpha_s^2/\mu^2$. We have used a typical value for $\mu = 0.50$ GeV. After the partons freeze out, they are traced back to their parent strings and are converted to hadrons using the Lund string fragmentation model [16].

Since the jet production cross section is small, we include additional hard jets in order to enhance statistics. The multiplicity of the additional jets in an event is obtained from a Poisson distribution with a mean $\langle n \rangle = 10$. The underlying dynamics of the base distribution ($dN_{\text{parton}}/dy \approx 250$ at $\sqrt{s} = 200A$ GeV) is not significantly affected by the smaller number of the embedded jets. This technique of oversampling has been widely used to study rare particle production, such as K^- at SIS/GSI [17], multistrange particles at SPS [18], and J/ψ at RHIC [19]. In $p + p$ collision, the lowest order (LO) pQCD momentum distribution of hard partons that propagate in the parton cascade is given by

$$E \frac{d\sigma_j^{pp}}{d^3p} = K \sum_{a,b} \int dx_a dx_b \int d^2\mathbf{k}_{T_a} d^2\mathbf{k}_{T_b} g(\mathbf{k}_{T_a}) g(\mathbf{k}_{T_b}) \times f_a(x_a, Q^2) f_b(x_b, Q^2) E \frac{d\sigma_{ab}}{d^3p}. \quad (2)$$

In Eq. (2), x_a, x_b are the momenta fractions and $\mathbf{k}_{T_a}, \mathbf{k}_{T_b}$ are the intrinsic transverse momenta of the initial

scattered partons. A constant factor $K = 2$ is used to account for the NLO corrections. For the collinear parton distribution function (PDF) $f_a(x_a, Q^2)$, we employ the LO Glück-Reya-Vogt (GRV94) parametrization [20], and for the transverse PDF $g(\mathbf{k}_{T_a})$, we use Gaussian intrinsic k_T distribution of width $\langle \mathbf{k}_{T_a}^2 \rangle = 1 \text{ GeV}^2/c^2$. We neglect nuclear shadowing for the jets as its effect is rather small at mid-rapidity at RHIC energies [21, 22]. Since we explore events with at least one triggered hadron of $p_T^{\text{trig}} > 4 \text{ GeV}/c$, a minimum momentum transfer of $p_T^{\text{min}} = 4 \text{ GeV}/c$ for the additional jets is assumed. In the hard processes, a proper formation time of $\tau_0 = 1/m_T$ is used for parton production with transverse mass m_T . The initial transverse coordinate of a hard jet is specified by the number of binary collision distribution for two Woods-Saxon geometries.

The hard jets can suffer energy loss by elastic scattering with the partons from HIJING. However, the dominant energy loss is via medium-induced gluon radiation along the trajectory of the jet. We consider here the dominant first-order total energy loss expression in opacity, $\chi = L/\lambda_g$, from the reaction operator approach [4, 23]:

$$\Delta E = 2\pi\alpha_s^3 C_a C_A \int_{\tau_0}^{\infty} d\tau \rho(\mathbf{r}(\tau), \tau) (\tau - \tau_0) \log \frac{2E}{\mu^2 L} . \quad (3)$$

Here, $\mathbf{r}(\tau)$ and E are the position and initial energy of the jet, $\rho(\mathbf{r}(\tau), \tau)$ is the parton density. The color factor C_a is given in Eq. (1) and may be expressed as $C_a = C_R C_T / d_A$, where C_R and C_T are the color Casimirs of the jet and the target parton, and d_A is the dimension in the adjoint representation with Casimir C_A . The effective path length required by the radiated gluons for traversing the matter, L , is taken to be 4 fm. Because of jet quenching the fragmentation function (FF) for a jet c to a hadron h in vacuum, $D_{h/c}(z_c, Q_c^2)$, is altered due to the modification of the kinetic variables of the jet, and the effective fragmentation function follows the relation [4],

$$z_c D'_{h/c}(z_c, Q_c^2) = z'_c D_{h/c}(z'_c, Q_{c'}^2) + N_g z_g D_{h/g}(z_g, Q_g^2) , \\ z_c = \frac{p_h}{p_c}, \quad z'_c = \frac{p_h}{p_c - \Delta E(p_c)}, \quad z_g = \frac{p_h}{\Delta E(p_c)/N_g} . \quad (4)$$

The second term on the right eventually gives the soft hadrons from the fragmentation of N_g radiated gluons. Note that the modified fragmentation function satisfies the sum rule $\int dz_c z_c D'_{h/c}(z_c, Q_c^2) = 1$. The initial hard jets after the partonic phase are fragmented using the LO Binnewies-Kniehl-Kramer (BKK) parametrization [24] of the fragmentation functions.

In absence of any definitive relation for how radiated energy should be translated into particles, we take recourse to a statistical prescription. Assuming local thermodynamical equilibrium of the parton medium, if $\Delta E(\mathbf{r}, \Delta\tau)$ is the energy radiated in a time interval $\Delta\tau$ (evaluated from Eq. (3)), the number of thermal gluons

emitted in $\Delta\tau$ can be related to the entropy increase ΔS of the plasma,

$$N_g(\mathbf{r}, \Delta\tau) \approx \frac{1}{4} \Delta S = \frac{1}{4} \frac{\Delta E(\mathbf{r}, \Delta\tau)}{T(\mathbf{r}, \tau)} , \quad (5)$$

where the local temperature $T \approx \epsilon(\mathbf{r}, \tau)/3\rho(\mathbf{r}, \tau)$ is extracted from the cascade by viewing the local parton number and energy densities $\rho(\mathbf{r}, \tau)$ and $\epsilon(\mathbf{r}, \tau)$. The factor of 1/4 comes from considering an ideal massless gas of classical particles in equilibrium. The radiated gluons are formed at space-time points along the parent jet's trajectory consistent with the energy loss described in Eq. (3). They are initially directed along the axis of the parent jet and subsequently scatter via elastic collision with the neighboring partons after a formation time τ_0 as used in HIJING. Effectively, this procedure converts 100% of the radiated energy into thermal energy, while maintaining momentum conservation. A less-efficient prescription for thermalizing the radiated energy would result in a reduced multiplicity. Based on local parton-hadron duality [25, 26], each of these radiated gluons after freeze-out are converted to a pion with equal probability for the three charge states.

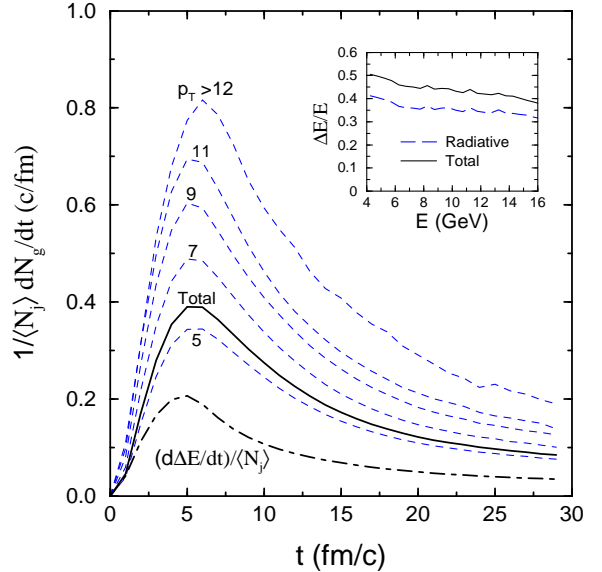


FIG. 1: The production rate of gluons at all rapidities from radiative jet energy loss in central ($b = 0 \text{ fm}$) Au+Au collisions at RHIC c.m. energy of $\sqrt{s} = 200A \text{ GeV}$. The results are for jets with different p_T (dashed lines) and for the total jets (solid line) in an event, normalized to the average number of jets $\langle N_j \rangle$ with the given p_T . The dash-dotted line gives the rate of radiative energy loss $(d\Delta E/dt)/\langle N_j \rangle$ in GeV/fm . The rise at small times is the result of performing the calculation in Cartesian time, rather than proper time. The inset shows the energy dependence of fractional energy loss $\Delta E/E$ of gluon jets due to radiation (dashed line) and after elastic scattering (solid).

The inset of Fig. 1 shows the fractional energy loss $\Delta E/E$ for the fast gluons traversing the partonic medium for central Au+Au collisions at a center of mass energy $\sqrt{s} = 200A$ GeV. In contrast to the asymptotic BDMS [2] energy loss for a thick static plasma, $\Delta E_{\text{BDMS}} = \pi \alpha_s^3 C_R C_A / 2 \cdot \tilde{v} \cdot L^2 \rho$ (the factor $\tilde{v} \propto \log(L/\lambda_g) \sim 1-3$), where $\Delta E/E$ increases rapidly with decreasing energy, the GLV [4, 23] first-order radiative energy loss ΔE (dashed line) exhibits almost a linear energy dependence for $E = 4-7$ GeV while at higher energy $\Delta E/E$ reveals a $\log(E)/E$ decrease. Elastic collision with other partons, which is modeled with the parton cascade, leads to an additional energy loss by 25% (solid line).

The dynamical evolution of the average energy loss per jet in an event (for jets at all rapidities), $(d\Delta E/dt)/\langle N_j \rangle$, rises for small times due to the longitudinal expansion of the system as shown in Fig. 1. If proper time had been used rather than Cartesian time, the rate would have monotonically fallen due to the falling density.

Figure 1 also shows the rapidity integrated dynamical rate of gluon radiation per average number of jets, $(dN_g/dt)/\langle N_j \rangle$, as evaluated from Eq. (5). The results are for total jets in an event, and also for jets with definite p_T . The emission pattern is found to follow that for the energy loss. Though the number of radiated gluons per $\langle N_j \rangle$ is seen to increase with p_T , the rapidly decreasing jet production cross section with increasing jet energy E actually leads to smallest number of gluon contribution from jets with $p_T \geq 12$ GeV/c. Although higher-energy jets are rare, they radiate more particles due to fact that they have more available energy and due to the logarithmic dependence of the radiation in Eq. (3). We find that partons with initial $p_T \sim 9$ GeV/c produce the bulk of the radiated gluons. Using the statistical prescription described above, about 5.5 soft gluons are emitted in an event per jet.

Since jets are typically formed in pairs, the observation of a jet can be used as a trigger. One can then search for the remains of the balancing jet, as well as any particle whose existence is derived from medium-induced radiation from the triggered jet. For our calculations, the trigger is defined as a hadron at midrapidity $|y| < 1$ with its transverse momentum p_T^{trig} above 4 GeV/c. The x direction is then defined to be perpendicular to the beam axis and pointing along the direction of the triggering hadron. Particles radiated from the trigger jet would typically have positive values of p_x while particles associated with the jet's partner would have negative values of p_x . For a perfect detector, momentum conservation implies

$$\int p_x \rho(p_x) dp_x = -P_T, \quad (6)$$

where $P_T \equiv p_T^{\text{trig}}$ is the momentum of the trigger particle and $\rho(p_x) = dN/dp_x$ refers to the momentum density of

all other particles. Of course, this constraint is significantly relaxed by finite acceptance. By making a similar distribution ρ_0 from other events, without the requirement of a trigger, one can define

$$\Delta\rho(p_x) = \rho(p_x) - \rho_0(p_x), \quad (7)$$

which describes the variation of the momentum density due to the jet. Two quantities related to $\Delta\rho$ are of particular interest:

$$\begin{aligned} \Delta N &\equiv \int \Delta\rho(p_x) dp_x, \\ \Delta P_x &\equiv \int p_x \Delta\rho(p_x) dp_x. \end{aligned} \quad (8)$$

ΔN counts the net number of additional particles, while ΔP_x describes the momentum, which should be a fraction of $-P_T$, determined by the acceptance.

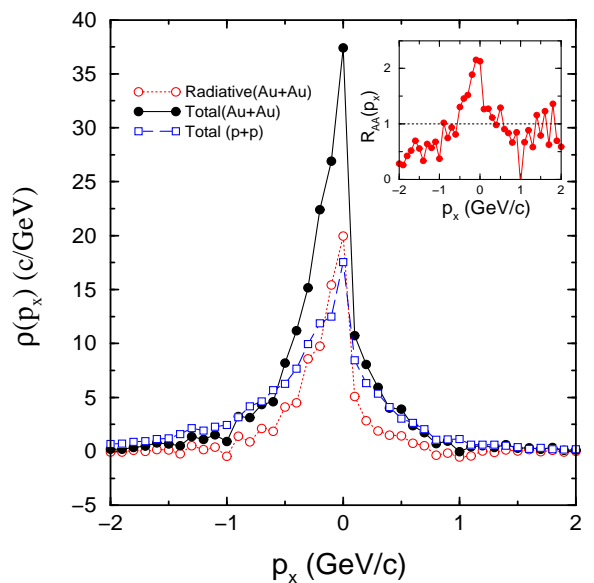


FIG. 2: The distribution $\rho(p_x)$ for particles produced at mid-rapidity $|y| < 1$ in events with a triggered hadron $4 < p_T^{\text{trig}} < 6$ GeV/c in the same rapidity range. The results are for total number of particles (solid circles) and for particles from radiative jet energy loss (open circles) in central ($b = 0$ fm) Au+Au collisions at RHIC energy of $\sqrt{s} = 200A$ GeV. The $p + p$ results at the same energy are shown by open squares. The ratio $R_{AA}(p_x)$ for the multiplicities in Au+Au collisions to that from $p + p$ collisions for the triggered jet event is shown in the inset.

Figure 2 shows $\rho(p_x)$ for events with a trigger momentum, $4 < P_T \equiv p_T^{\text{trig}} < 6$ GeV/c. For large negative values of p_x , $\rho(p_x)$ is suppressed in Au+Au collisions relative to $p + p$ results as expected due to the suppression of away-side jets [11]. The situation is reversed for $|p_x| < 600$ MeV/c, where the spectrum is dominated by the radiated and rescattered particles. The momentum

constraint, Eq. (6), is satisfied by an increase of low momentum particles to compensate for the loss of the away-side jet. The net number of extra particles, ΔN , is higher in the Au+Au case as would be expected from the induced-radiation and from the statistical nature of Eq. (5) which converts the radiated energy into particles with momenta characterized by the temperature. The alteration of the jets is especially apparent in the inset of Fig. 2 which shows the ratio of the Au+Au and pp results. At large negative p_x the suppression is approximately a factor of 3, while the enhancement at low p_x is approximately a factor of two.

Also shown in Fig. 2 (open circles) is the distribution of the particles in Au+Au collisions that stems from the induced radiation described in Eq. (3). As expected, these particles are at much lower p_T than those from pp collisions due to their thermalizing with the medium.

For this range of triggers the number of extra particles, both charged and neutral, produced at mid-rapidity was approximately $\Delta N = 19$, versus 14 for pp collisions. We emphasize that this is a relative increase and that determining ρ_0 is difficult, as discussed later. The numbers increase by $\sim 20\%$ if all rapidities are evaluated. Of course, experiments would detect a reduced number after accounting for efficiencies and acceptances. By itself, this number provides important insight into the driving force behind the disappearance of away-side jets. If the disappearance of away-side jets was largely an initial-state effect, e.g., $2 \rightarrow 1$ gluon fusion processes in the gluon saturation model [12], few extra particles would be created, especially at mid-rapidity. One would then expect to see a reduction in ΔN for Au+Au vs pp rather than the increase found here.

If we assume a perfect detector, the momentum integration described in Eqs. (6) and (8), resulted in $\Delta P_x = -4.2$ GeV/c, after triggering on leading hadrons in the $p_T^{\text{trig}} = 4-6$ GeV/c range. This verifies momentum conservation in the procedure. As with the calculation of ΔN , most of this balancing momentum was found in the mid-rapidity cut. If the mechanism for jet quenching were an initial-state effect, one would expect less of the balancing momentum to be found with a rapidity near that of the triggering hadron.

It would be straight-forward to expand this analysis to include a binning in rapidity as well as p_x . One could then analyze the degree to which a jet spreads its energy and momentum in rapidity. Another possibility would be to bin with p_T or E_T which would allow the determination of the extra energy related to the trigger. The calculations shown here were performed with approximately 4×10^4 trigger particles. Two-dimensional binnings would require significantly higher statistics. We would certainly expect large-acceptance experiments such as STAR or PHENIX to be able to perform a comparable analysis as to what was demonstrated here if they were able to measure on the order of 10^5 events with trigger particles.

Given sufficient statistics, the principal difficulty of these sort of analyses lies in defining a class of similar events for the purpose of background subtraction. For instance, if one uses multiplicity at mid-rapidity to define the events, the quantity ΔN would always be zero. The means for determining centrality must be independent of the particles used in the analysis of ρ and ρ_0 . Furthermore, it must be sufficiently accurate so that the observation of the triggering jet does not bias the event towards being more central. It might be quite possible to quantitatively estimate and correct for such a bias. Fortunately, these effects do not determine the extraction of ΔP_x since the base distribution, ρ_0 does not contribute to P_x .

We also investigated the degree to which our predictions are sensitive to the parameters used in the model. By reducing the medium-induced energy loss by a factor of two, the net number of extra radiated particles was only reduced from 5.5 to about half that number. The energy loss is found to be rather insensitive to the parton elastic cross section. Once the medium becomes opaque, the behavior should be fairly insensitive to details as thermalization should mask any details of the microscopic physics, and the linear dependence of the induced multiplicity with the energy loss parameters should dampen. Consequently, with a much higher initial gluon density, e.g., $dN_g/dy \approx 1000$ is suggested in some gluon saturation models [25], it is not clear to what degree the distribution of produced particles would be increased.

In conclusion, we have shown that an analysis of low p_T observables can unveil the fate of lost jets at RHIC. A similar analysis of experimental data could provide irrefutable evidence for establishing final-state jet energy loss as the explanation for jet suppression. A high-statistics multi-dimensional analysis would provide quantitative insight into the dynamics and dissipation of jets in high-density matter.

The authors wish to thank Ivan Vitev for explaining the finer points of medium-induced radiation. This work was supported by the National Science Foundation under Grant No. PHY-0070818.

- [1] M. Gyulassy and X.N. Wang, Nucl. Phys. **B420** (1994) 583.
- [2] R. Baier, Y.L. Dokshitzer, A.H. Mueller, and D. Schiff, Nucl. Phys. **B484** (1997) 265; Phys. Rev. C **58** (1998) 1706.
- [3] U.A. Wiedemann Nucl. Phys. **B582** (2000) 409; Nucl. Phys. **B588** (2000) 303.
- [4] M. Gyulassy, P. Léval, and I. Vitev, Nucl. Phys. **B594** (2001) 371; **B571** (2001) 197; M. Gyulassy, I. Vitev, X.N. Wang, Phys. Rev. Lett. **86** (2001) 2537; M. Gyulassy, I. Vitev, X.N. Wang, and B.W. Wang, nucl-th/0302077.

- [5] E. Wang and X.N. Wang, Phys. Rev. Lett. **89** (2002) 162301; I. Vitev and M. Gyulassy, Phys. Rev. Lett. **89** (2002) 252301;
- [6] T. Hirano and Y. Nara, Phys. Rev. C **66** (2002) 041901; nucl-th/0301042.
- [7] K. Adcox et al., PHENIX Collaboration, Phys. Rev. Lett. **88** (2002) 022301; S.S. Adler et al., PHENIX Collaboration, nucl-ex/0304022, hep-ex/0304038, nucl-ex/0306021.
- [8] C. Adler et al., STAR Collaboration, Phys. Rev. Lett. **89** (2002) 202301; J. Adams et al., STAR Collaboration, nucl-ex/0305015.
- [9] B.B. Back et al., PHOBOS Collaboration, nucl-ex/0302015.
- [10] I. Arsene et al., BRAHMS Collaboration, nucl-ex/0307003.
- [11] C. Adler et al., STAR Collaboration, Phys. Rev. Lett. **90** (2003) 082302.
- [12] D. Kharzeev, E. Levin, and L. McLerran, Phys. Lett. B **561** (2003) 93.
- [13] M. Gyulassy and X.N. Wang, Comp. Phys. Comm. **83**, (1994) 307; X.N. Wang and M. Gyulassy, Phys. Rev. D **44** (1991) 3501.
- [14] Z.W. Lin, S. Pal, C.M. Ko, B.A. Li, and B. Zhang, Phys. Rev. Phys. Rev. C **64** (2001) 011902.
- [15] B. Zhang, Comp. Phys. Comm. **109** (1998) 193; M. Gyulassy, Y. Pang and B. Zhang, Nucl. Phys. **A626** (1997) 999.
- [16] B. Andersson, G. Gustafson, G. Ingelman and T. Sjöstrand, Phys. Rep. **97** (1983) 31; B. Andersson, G. Gustafson and B. Soderberg, Z. Phys. C **20** (1983) 317.
- [17] J. Randrup and C.M. Ko, Nucl. Phys. **A343** (1980) 519.
- [18] S. Pal, C.M. Ko, and Z.-W. Lin, nucl-th/0106073.
- [19] B. Zhang, C.M. Ko, B.-A. Li, Z.-W. Lin, and S. Pal, Phys. Rev. C **65** (2002) 054909.
- [20] M. Glück, E. Reya, and W. Vogt, Z. Phys. C **67** (1995) 433.
- [21] S. Jeon, J. Jalilian-Marian, and I. Sarcevic, Phys. Lett. B **562** (2003) 45.
- [22] S.R. Klein and R. Vogt, Phys. Rev. C **67** (2003) 047901.
- [23] M. Gyulassy, P. Levai, and I. Vitev, Phys. Rev. Lett. **85** (2000) 5535.
- [24] J. Binnewies, B.A. Kniehl, and G. Kramer, Z. Phys. C **65** (1995) 471.
- [25] K.J. Eskola, K. Kajantie, P.V. Ruuskanen, and K. Tuominen, Nucl. Phys. **B570** (2000) 379.
- [26] D. Molnár and M. Gyulassy, Nucl. Phys. **A697** (2002) 495.